



Simplified optical correlation-domain reflectometry employing proximal reflection point

Makoto Shizuka¹, Heeyoung Lee¹, Neisei Hayashi², Yosuke Mizuno^{1*}, and Kentaro Nakamura¹

¹*Institute of Innovative Research, Tokyo Institute of Technology, Yokohama 226-8503, Japan*

²*Research Center for Advanced Science and Technology, The University of Tokyo, Meguro, Tokyo 153-8904, Japan*

*E-mail: ymizuno@sonic.pi.titech.ac.jp

Received August 9, 2016; accepted October 9, 2016; published online November 16, 2016

We develop a new configuration of simplified optical correlation-domain reflectometry using a proximal reflection point. The experimental setup is basically composed of standard silica fibers and includes neither an optical frequency shifter such as an acousto-optic modulator nor an explicit reference path. The light reflected at the proximal reflection point, which is artificially fabricated near an optical circulator, is used as the reference light. Unlike the conventional silica-based setup, this configuration can perform a distributed reflectivity measurement along the distal half of the sensing fiber. After demonstration of the basic operation, the incident optical power dependence of the reflectivity distribution is investigated, and the existence of the optimal incident power is clarified. © 2016 The Japan Society of Applied Physics

Fiber-optic distributed reflectometry has been vigorously studied as one of the key methods for developing smart materials and structures.¹⁻⁴ Among various types of reflectometry, those based on Fresnel reflection enable us to detect bad connections (or splices) and other reflection points along fibers under test (FUTs) in a distributed manner. Two of its successful configurations are optical time-domain reflectometry (OTDR)⁵⁻⁹ and optical frequency-domain reflectometry (OFDR),¹⁰⁻¹⁴ both of which have the limitations of insufficient spatial resolution and relatively low measurement speed, and phase fluctuations caused by environmental disturbance, respectively. To mitigate these shortcomings, optical correlation (or coherence)-domain reflectometry (OCDR)¹⁵⁻²⁵ based on a synthesized optical coherence function (SOCF)²² has been developed and extensively studied. Among the many SOCF-OCDR configurations using directly modulated laser outputs¹⁷⁻²² and optical frequency combs,^{23,24} those based on direct sinusoidal modulation of the laser outputs¹⁷⁻¹⁹ can be most cost-efficiently implemented.

To further reduce the implementation cost and boost convenience in practical applications, we have been focusing on the simplification of the SOCF-OCDR systems by sinusoidal modulation. First, by exploiting the foot of the Fresnel reflection spectrum, we developed a configuration that did not require an optical frequency shifter such as an acousto-optic modulator (AOM).²⁶ We subsequently implemented this AOM-free SOCF-OCDR without using an explicit reference path.²⁷ In this configuration, the Fresnel-reflected light generated at the distal open end of an FUT [silica single-mode fiber (SMF)] was exploited as the reference light. This configuration, however, poses two problems: 1) the measurement range is limited to the proximal half of the FUT length and 2) the measurement cannot be continued when the FUT has even one breakage point. In order to alleviate these problems, a polymer optical fiber (POF) was used as an FUT in the same configuration without a reference path,²⁸ which enables us to exploit the Fresnel reflection at the proximal boundary between the silica SMF and the POF (instead of that at the distal open end of the FUT). The reflectivity measurement along the distal half of the FUT, which is more convenient for practical applications, was successfully demonstrated. Besides, the measurement was not interrupted even when part of the FUT was broken. However, the use of non-silica fibers is not ideal in some cases, because they

are not compatible with the fiber-optic telecommunication systems, which are usually composed of silica SMFs.

In this work, we develop a new silica-SMF-based configuration of AOM-free SOCF-OCDR without an explicit reference path. As the reference light, we use the Fresnel-reflected light at a partial reflection point artificially produced near an optical circulator. A distributed reflectivity measurement along the distal half of the FUT is demonstrated, and then the incident optical power dependence of the reflectivity distribution is investigated.

In general, distributed reflectivity measurements by SOCF-OCDR using explicit reference paths (either with or without an AOM) are performed on the basis of optical correlation control.²⁶ Specifically, the optical frequency of the laser output is sinusoidally modulated to generate what is called a correlation peak in the FUT.²² By controlling modulation frequency, the position of the correlation peak can be scanned along the FUT, and thus the reflected light can be measured in a distributed manner. On account of the periodicity of correlation peaks, the measurement range D of standard SOCF-OCDR systems is determined by their interval as

$$D = \frac{c}{2nf_m}, \quad (1)$$

where c is the optical velocity in a vacuum, n is the core refractive index, and f_m is the modulation frequency of the laser output. The bandwidth of the correlation peak determines the spatial resolution Δz as

$$\Delta z \cong \frac{0.76c}{\pi n \Delta f}, \quad (2)$$

where Δf is the modulation amplitude.

Subsequently, consider the performance of reference-path-free SOCF-OCDR systems. As described in detail in Ref. 27, when the Fresnel-reflected light at the open end of the FUT is used as the reference light, the measurement range is limited only to the proximal half of the FUT [not determined by Eq. (1)]. Here, we instead produce an artificial reflection point at the proximal end of the FUT (near an optical circulator) and suppress the reflection at the distal end. Then the Fresnel-reflected light at the proximal end of the FUT can be used as a reference light. In this case, the zeroth-order correlation peak (i.e., the zero-optical-path-difference point) is constantly located at the proximal reflection point, and the

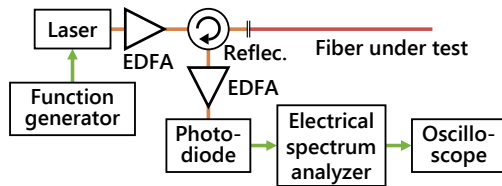


Fig. 1. (Color online) Experimental setup of the silica-based reference-path-free SOCF-OCDR system. EDFA, erbium-doped fiber amplifier.

first-order correlation peak is exploited for distributed measurement. Considering that the second-order correlation peak starts to enter the FUT at the distal end of the FUT when the first-order correlation peak is scanned from the distal end to the midpoint, the measurement range is limited to the distal half of the FUT. This operating principle has been described in more detail in the case of a POF-based system.²⁸⁾ Note that a similar configuration has also been reported in Brillouin-based OCDR systems.^{29,30)}

The experimental setup of the reference-path-free SOCF-OCDR is shown in Fig. 1. All the optical paths were mainly composed of silica SMFs. The output of a laser at 1.55 μm with a 3 dB bandwidth of ~1 MHz was amplified using an erbium-doped fiber amplifier (EDFA) and was injected into the FUT via an optical circulator. The light reflected from the FUT was amplified to ~3 dBm using another EDFA. The optical beat signals of this reflected light and the Fresnel-reflected light were converted to electrical signals using a photo diode and was sent to an electrical spectrum analyzer (ESA). The resolution bandwidth and video bandwidth of the ESA were set to 300 and 1 kHz, respectively. To enable high-speed operation, the spectral power at 2 MHz [with a maximal signal-to-noise ratio (SNR)]²⁶⁾ was continuously output from the analog terminal of the ESA to an oscilloscope.

The proximal partial reflection point was, in this experiment, composed of a 650-μm-long air gap filled with cyclic transparent optical polymer (CYTOP) liquid, which has been used as the core material for perfluorinated graded-index POFs with a relatively low propagation loss (~250 dB/km at 1.55 μm).^{31–33)} The reflection point was fabricated between the open end of a 1-m-long pigtail (silica SMF; second port) of the optical circulator and the proximal end of the FUT. The structure of the FUT is shown in Fig. 2, where 7-, 5-, 4-, and 3-m-long silica SMFs were sequentially connected using “ferrule connector/physical contact (FC/PC)” connectors (loosely connected to imitate weak reflection points). The distal PC end of the FUT was kept open. The modulation amplitude Δ*f* was 3.9 GHz and the modulation frequency was swept from 5.15 to 10.3 MHz, corresponding to the nominal spatial resolution of ~30 mm according to Eq. (2), which is >40 times larger than the gap of the partial reflection point. The repetition rate was 20 Hz, and averaging was performed 32 times.

Figure 3 shows the measured reflection power distribution along the distal half of the FUT when the incident power was 0 dBm. The horizontal axis indicates the distance from the reflection point where the 0th correlation peak was located. The three weak reflection points, including the open end, were successfully detected at the correct positions. Note that because of the total loss of the proximal reflection points is high, the light reflected at the distal open end of the FUT

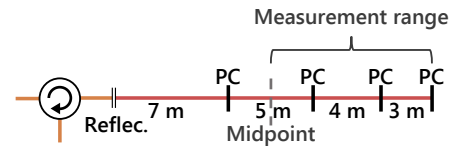


Fig. 2. (Color online) Structure of the fiber under test.

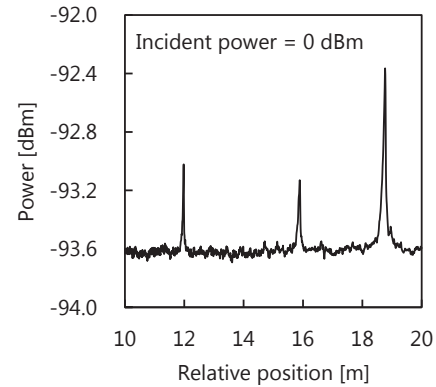


Fig. 3. Reflection power distribution measured along the distal half of the FUT. The incident power was 0 dBm. The horizontal axis indicates the distance from the reflection point where the 0th correlation peak was located.

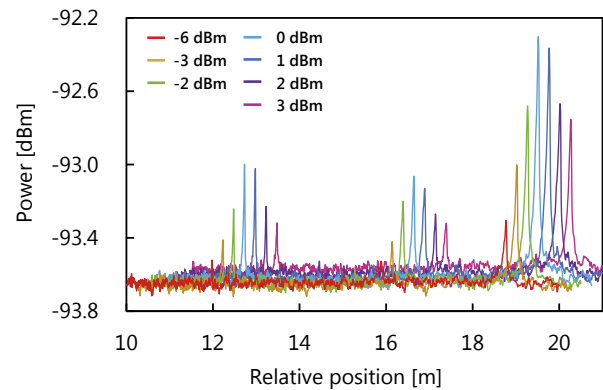


Fig. 4. (Color online) Reflectivity distributions measured at various incident powers from –6 to 3 dBm. Each distribution is shifted by 0.25 m; the horizontal scale is true only for the result at –6 dBm.

becomes relatively low in power, and thus cannot serve as the reference light.

We then measured the incident optical power dependence of the reflectivity distribution. Figure 4 shows the reflectivity distributions at various incident powers from –6 to 3 dBm. Each result is shifted by 0.25 m. The power of each peak increased when the incident power was increased from –6 to 0 dBm, but it decreased when the incident power was further increased. Here, we define the SNR of each peak detection as the difference between the peak power and the noise floor (the power at a position of 14 m was used). Figure 5 shows the SNRs of the each peak plotted as functions of the incident optical power. Irrespective of the peaks, the SNR was maximal when the incident power was 0 dBm. This behavior is the same as that reported in Ref. 27. Thus, the optimal incident power was shown to exist from the viewpoint of the SNR.

In conclusion, a new configuration of AOM-free SOCF-OCDR without an explicit reference path was implemented using a silica SMF as the FUT. A proximal partial reflection

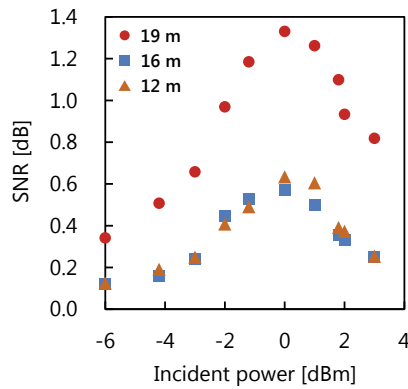


Fig. 5. (Color online) Incident optical power dependence of the SNR of the three peaks at the relative positions of 12, 16, and 19 m.

point was artificially fabricated near an optical circulator, and the light reflected at this point was used as a reference light. The measurement capability of a distributed reflectivity measurement along the distal half of the FUT was experimentally proved. In addition, the incident optical power dependence of the reflectivity distribution was investigated, and the existence of the optimal incident power was clarified. We anticipate that our silica-based AOM-free SOCF-OCDF system without an explicit reference path will be of great use for implementing cost-effective distributed reflectivity sensors in the near future.

Acknowledgments This work was supported by JSPS KAKENHI Grant Numbers 25709032, 26630180, and 25007652, and by research grants from the Iwatani Naoji Foundation, the SCAT Foundation, and the Konica Minolta Science and Technology Foundation.

1) C. K. Y. Leung, K. T. Wan, D. Inaudi, X. Bao, W. Habel, Z. Zhou, J. Ou, M. Ghandehari, H. C. Wu, and M. Imai, *Mater. Struct.* **48**, 871 (2015).

2) A. Barrias, J. R. Casas, and S. Villalba, *Sensors* **16**, 748 (2016).
 3) W. Zou, S. Yang, X. Long, and J. Chen, *Opt. Express* **23**, 512 (2015).
 4) Y. Mizuno, N. Hayashi, H. Fukuda, K. Y. Song, and K. Nakamura, *Light: Sci. Appl.* **5**, e16184 (2016).
 5) M. K. Barnoski and S. M. Jensen, *Appl. Opt.* **15**, 2112 (1976).
 6) G. P. Lees, H. H. Kee, and T. P. Newson, *Electron. Lett.* **33**, 1080 (1997).
 7) M. Zoboli and P. Bassi, *Appl. Opt.* **22**, 3680 (1983).
 8) P. Healey and P. Hensel, *Electron. Lett.* **16**, 631 (1980).
 9) Q. Zhao, L. Xia, C. Wan, J. Hu, T. Jia, M. Gu, L. Zhang, L. Kang, J. Chen, X. Zhang, and P. Wu, *Sci. Rep.* **5**, 10441 (2015).
 10) W. Eickhoff and R. Ulrich, *Appl. Phys. Lett.* **39**, 693 (1981).
 11) D. Uttam and B. Culshaw, *J. Lightwave Technol.* **3**, 971 (1985).
 12) B. J. Soller, D. K. Gifford, M. S. Wolfe, and M. E. Froggatt, *Opt. Express* **13**, 666 (2005).
 13) S. Venkatesh and W. V. Sorin, *J. Lightwave Technol.* **11**, 1694 (1993).
 14) F. Ito, X. Fan, and Y. Koshikiya, *J. Lightwave Technol.* **30**, 1015 (2012).
 15) R. C. Youngquist, S. Carr, and D. E. N. Davies, *Opt. Lett.* **12**, 158 (1987).
 16) E. A. Swanson, D. Huang, M. R. Hee, J. G. Fujimoto, C. P. Lin, and C. A. Puliafito, *Opt. Lett.* **17**, 151 (1992).
 17) K. Hotate, M. Enyama, S. Yamashita, and Y. Nasu, *Meas. Sci. Technol.* **15**, 148 (2004).
 18) Z. He, T. Tomizawa, and K. Hotate, *IEICE Electron. Express* **3**, 122 (2006).
 19) Z. He, M. Konishi, and K. Hotate, *Proc. SPIE* **7004**, 70044L (2008).
 20) K. Hotate and O. Kamatani, *Electron. Lett.* **25**, 1503 (1989).
 21) Z. He and K. Hotate, *J. Lightwave Technol.* **20**, 1715 (2002).
 22) K. Hotate, *Meas. Sci. Technol.* **13**, 1746 (2002).
 23) Z. He, H. Takahashi, and K. Hotate, *CLEO2010, 2010, CFH4*.
 24) H. Takahashi, Z. He, and K. Hotate, *ECOC2010, 2010, Tu.3.F.4*.
 25) T. Okamoto, D. Iida, K. Toge, and T. Manabe, *J. Lightwave Technol.* **34**, 4259 (2016).
 26) M. Shizuka, S. Shimada, N. Hayashi, Y. Mizuno, and K. Nakamura, *Appl. Phys. Express* **9**, 032702 (2016).
 27) M. Shizuka, N. Hayashi, Y. Mizuno, and K. Nakamura, *Appl. Opt.* **55**, 3925 (2016).
 28) N. Hayashi, M. Shizuka, K. Minakawa, Y. Mizuno, and K. Nakamura, *IEICE Electron. Express* **12**, 20150824 (2015).
 29) N. Hayashi, Y. Mizuno, and K. Nakamura, *IEEE Photonics J.* **7**, 6800407 (2015).
 30) N. Hayashi, Y. Mizuno, and K. Nakamura, *IEEE Photonics J.* **6**, 6803108 (2014).
 31) Y. G. Zhao, W. K. Lu, Y. Ma, S. S. Kim, S. T. Ho, and T. J. Marks, *Appl. Phys. Lett.* **77**, 2961 (2000).
 32) Y. Koike and M. Asai, *NPG Asia Mater.* **1**, 22 (2009).
 33) Y. Mizuno and K. Nakamura, *Appl. Phys. Lett.* **97**, 021103 (2010).